chemosensors

Article

Resolution of Glycerol, Ethanol and Methanol Employing a Voltammetric Electronic Tongue

João Pedro Jenson de Oliveira [1,2,3], Marta Bonet-San-Emeterio [3], Acelino Cardoso de Sá [4], Xavier Cetó [3], Leonardo Lataro Paim [2] and Manel del Valle [3,*]

[1] School of Electrical and Computer Engineering, University of Campinas (UNICAMP), Campinas 13083-852, São Paulo, Brazil; joao.jenson@unesp.br
[2] Department of Energy Engineering, São Paulo State University (UNESP), Rosana 192740-000, São Paulo, Brazil; leonardo.paim@unesp.br
[3] Sensors and Biosensors Group, Department of Chemistry, Universitat Autònoma de Barcelona (UAB), Edifici Cn, Bellaterra, 08193 Barcelona, Spain; martabonetsanemeterio@gmail.com (M.B.-S.-E.)
[4] Department of Physics and Materials Science, University of São Paulo (USP), São Carlos 13566-590, São Paulo, Brazil; acelino2@hotmail.com
* Correspondence: manel.delvalle@uab.cat

Abstract: This paper reports the use of nanoparticles (NPs)-modified voltammetric sensors for the rapid determination of glycerol in the presence of ethanol and methanol, which are used in the transesterification reaction of biodiesel production. Two different modified electrodes have been prepared to form the electronic tongue (ET): copper hexacyanoferrate NPs obtained by chemical synthesis and mixed into graphite/epoxy (GEC) electrode, and nickel hydroxide NPs electrodeposited in reduced graphene oxide onto a GEC electrode. The response characteristics of these electrodes were first evaluated by building the respective calibration against glycerol, ethanol, and methanol. The electrodes demonstrated good stability during their analytical characterization, while principal component analysis confirmed the differentiated response against the different alcohols. Finally, the quantification of mixtures of these substances was achieved by a genetic algorithm-artificial neural networks (GA-ANNs) model, showing satisfactory agreement between expected and obtained values.

Keywords: electronic tongue; nanoparticles modifiers; glycerol; biodiesel; artificial neural networks

Citation: de Oliveira, J.P.J.; Bonet-San-Emeterio, M.; de Sá, A.C.; Cetó, X.; Paim, L.L.; del Valle, M. Resolution of Glycerol, Ethanol and Methanol Employing a Voltammetric Electronic Tongue. *Chemosensors* **2024**, *12*, 173. https://doi.org/10.3390/chemosensors12090173

Received: 19 July 2024
Revised: 27 August 2024
Accepted: 30 August 2024
Published: 1 September 2024

1. Introduction

Biodiesel, a renewable biomass-derived biofuel intended for use in internal combustion engines, is synthesized through a chemical process known as transesterification [1,2]. The production of biodiesel entails the use of vegetable or animal oils in combination with short-chain alcohols such as methanol or ethanol. This reaction can be catalyzed by either an acid or a base, although the basic route is generally preferred due to its capacity to yield higher conversion rates [2,3]. The most frequently employed catalysts in this process are sodium and potassium hydroxides. Consequently, residual catalysts may persist in the biodiesel due to the inefficacy of the product purification methods [4].

In conjunction with biodiesel production through the transesterification reaction, another byproduct emerges: glycerol. Glycerol, classified as an organic alcohol [5], is inherently present in all animal and plant-derived oils and fats, predominantly in a combined form, where it is bound to fatty acids. However, the presence of glycerol poses challenges for engines, as it can lead to the accumulation of residues at the injector nozzles, in the depths of vehicle fuel tanks, and even cause complications in storage systems [6]. Another significant concern pertains to the combustion of biodiesel in the presence of glycerol (occurring at temperatures exceeding 180 °C), resulting in the formation of acrolein, a highly detrimental compound for both human health and the environment [7].

Consequently, the quantification of glycerol residues within biodiesel is of paramount importance not only for the optimal performance of this biofuel, but also to prevent the incineration of deleterious byproducts that pose risks to human health [4,7]. Even more, accurately assessing the levels of residues within biodiesel represents the first step towards addressing its removal. Hence, there arises a need to develop sensitive and reliable analytical techniques for the quantification of glycerol in biodiesel [6,8].

Among analytical methods, electrochemical methods involving the use of sensors modified with nanomaterials have garnered significant attention in the literature [9,10]. This is because they have introduced innovations and substantial improvements to traditional analytical methods, offering numerous advantages. The primary distinctions and innovations of electrochemical sensors with nanomaterials include faster response time, enhanced sensitivity, lower detection limits, or higher compound selectivity, among other factors [9,10]. Overall, electrochemical sensors with nanomaterials offer a wide array of advantages and innovations, which have led to their adoption in diverse fields, including environmental monitoring, healthcare, food safety, and industrial process control [11,12].

In this context, several researchers have been actively engaged in refining the detection of contaminants in biodiesel using electrochemical sensors [13]. For instance, Arévalo et al. developed a sensitive electrochemical sensor for glycerol detection in biodiesel samples using copper oxide nanoparticles (NPs)-decorated multiwalled carbon nanotubes/pectin composite deposited onto a glassy carbon electrode (GCE) [14]. Another interesting example is the method proposed by Honório et al., involving electrochemical detection and solid phase extraction [15]; researchers used solid-phase extraction to isolate free glycerol from other components, while electrochemical analysis was conducted using palladium-modified GCE, making it a cost-effective and faster alternative to GC-based techniques. Similarly, Magno et al. reported the modification of a GCE with reduced graphene oxide and core-shell gold@palladium nanoparticles for the determination of glycerol in the aqueous phase obtained after liquid–liquid extraction from a biodiesel sample [16]. In another study, the combination of a GCE with electrochemically reduced graphene and electrochemically deposited gold nanoparticles was also applied for the determination of free glycerol in biodiesel previously extracted by liquid phase extraction [17]. Lastly, Ravipati et al. recently reported the use of copper–metal–organic framework (Cu-MOF) as a versatile electrocatalyst for detecting glycerol in biodiesel [18].

However, while individual sensors may excel in the discrete analysis of specific compounds, their efficacy diminishes when faced with complex matrices comprising multiple constituents. In such instances, the need arises for alternative technologies capable of simultaneous compound detection. Within the realm of sensor technology, an innovative approach emerged, characterized by the incorporation of sensor arrays alongside intricate data processing methodologies, colloquially referred to as electronic tongue (ET). ETs represent highly adaptable sensor systems, adept at simultaneous monitoring of diverse analyte concentrations. They excel not only in scrutinizing analytes amidst the presence of their interfering agents, but also in the disentanglement of a mixture of similar analytes [19–21].

An ET, fundamentally, constitutes a multi-sensory arrangement featuring a suite of sensors that exhibit modest selectivity, along with advanced signal processing in the realms of pattern recognition and multivariate data analysis, to distill significance from the intricacies of this complex dataset [19]. In other words, ETs comprise an assemblage of sensors to generate multidimensional insights, supported by chemometric processing tools such as artificial neural networks (ANNs) or principal component analysis (PCA), among others, and serve as a pivotal analytical apparatus tailored for the analysis of complex liquid samples. To the best of the authors' knowledge, although chemometric tools have been applied to the analysis of biodiesel, the application of a voltammetric ET for the analysis of glycerol in biodiesel has not been reported so far [22–24].

In this direction, the present work tackles the characterization and application of a voltammetric ET for the analysis of glycerol, ethanol, and methanol, three relevant byproducts in the production of biodiesel. The developed ET is based on an array of graphite-epoxy

composite (GEC) electrodes modified with different metal oxide NPs (viz., nickel and copper); some of these electrodes were previously used in analysis of monosacharides [25]. The response of the developed electrodes was first characterized against the three alcohols individually, confirming its good performance and differentiated sensitivity and selectivity towards the alcohols under scrutiny. Next, an ANN quantitative model for the simultaneous quantification of the different compounds was built by combining the responses of the different electrodes. However, due to the inherent high dimensionality of the data considered, a preprocessing stage employing genetic algorithms (GAs) was employed to select the more relevant features and improve the model performance and generalization ability. This integration of NPs-modified electrodes and advanced data processing facilitated the discernment of complex chemical constituents within the tested alcohols, empowering the system to distinguish between them with a remarkable degree of precision.

2. Materials and Methods

2.1. Chemicals and Reagents

All chemical reagents employed in this study were of analytical-grade quality. Aqueous solutions were prepared using deionized water derived from a Milli-Q system, as provided by Millipore, based in Billerica, MA, USA. Nickel(II) nitrate hexahydrate (≥99.999%), copper(II) nitrate pentahydrate (99.99%), potassium(III) hexacyanoferrate (≥99%), potassium chloride (≥99%), potassium nitrate (≥99%), potassium sulfate (≥99%), monobasic potassium phosphate (≥99%), dibasic potassium phosphate (≥98%), and sodium hydroxide (≥97%) were all procured from Sigma-Aldrich (St. Louis, MO, USA). Sulfuric acid (≥95%), sodium nitrate (≥99%), and potassium permanganate (≥99%) were purchased from Merck (Darmstadt, Germany). Hydrochloric acid (≥37%) was obtained from Panreac Química (Barcelona, Spain). Glycerol (≥99.5%), in its pure form, was sourced from Acros Organics, a division of Thermo Fisher Scientific, situated in Geel, Belgium. Methanol (≥99.8%) and ethanol (≥99.5%) were acquired from Scharlau (Barcelona, Spain). The Resineco epoxy kit resin was provided by Resineco Green Composites, a company based in Barcelona, Spain. Additionally, graphite powder was purchased from BDH Laboratory Supplies, located in Poole, UK.

2.2. Apparatus and Measurements

The amperometric measurement cell consisted of two metal NPs-modified GEC electrodes (see Section 2.3), along with an ORP reference Ag/AgCl electrode (Fisher Scientific, Madrid, Spain). For the acquisition of data through cyclic voltammetry, a 6-channel AUTOLAB PGSTAT20 potentiostat, manufactured by Ecochemie in the Netherlands, was used. The potentiostat was configured in a multichannel arrangement and commanded by the provided GPES Multichannel 4.7 software package. Voltammetric measurements encompassed electrode potentials ranging from −1.0 V to +1.0 V (versus Ag/AgCl), accomplished with a scan rate of 100 mV/s. It is pertinent to note that all electroanalytical experiments were conducted at room temperature.

2.3. Electrodes Preparation

2.3.1. Graphene Synthesis

Graphene oxide (GO, 5 mg/mL) was synthesized through a modified version of the Hummers method [26,27]. Briefly, graphite and sodium nitrate are mixed with sulfuric acid previously cooled to 0 °C, followed by the slow addition of potassium permanganate to the previous flask to avoid excessive heating. Next, the mixture was stirred for 4 h at room temperature, plus 30 min at 35 °C. The end of the oxidation process was conducted under controlled temperature conditions by adding deionized water into the reaction and maintaining the solution at 70 °C under stirring for 15 min. Finally, the obtained graphene oxide was separated and purified. The synthesized graphene oxide was previously characterized in other studies; however, additional characterizations are provided in the Supplementary Information of this work.

2.3.2. Copper NPs Synthesis

Copper hexacyanoferrate (CuHCF) NPs were synthesized by a facile coprecipitation method based on a previously reported procedure [28]. Initially, a 10 mM solution of potassium ferrocyanide and a 10 mM solution of copper nitrate were separately prepared in MilliQ water (100 mL each), and then heated up to 50 °C. Then, the $Cu(NO_3)_2$ solution was slowly pumped (0.28 mL/min) for 6 h to the $K_3Fe(CN)_6$ solution (under constant stirring at 500 rpm), leading to the formation and precipitation of NPs. Finally, the obtained precipitate was filtered with a 0.20 µm Millipore's Omnipore membrane purchased from Merck (Darmstadt, Germany), completely washed with ethanol and pure water, and dried at 70 °C under vacuum for 3 days.

2.3.3. Preparation of GECs

The electrode assembly process started with the integration of a PVC tube body, adjoined with a copper disk that was affixed at an electrical connector, as previously described [29]. After the assembly, a composite of graphite and epoxy (GEC) material was concocted. This mixture was prepared through manual blending of the epoxy resin, the hardener, and graphite powder. The resultant slurry underwent a homogenization process, after which the paste was inserted into the PVC tubes and then subjected to a curing process at 40 °C for two days. Upon completion of the curing phase, the electrodes underwent a polishing procedure using sandpaper in successive grain sizes of 300, 600, 800, and 1200 until the attainment of a uniform electrode surface.

2.3.4. Preparation of Modified GECs

The CuHCF NPs-modified electrodes were prepared in the same way as the graphite working electrodes. The powder obtained by the chemical synthesis was mixed with the substrate composite in a ratio of 5% of the amount of graphite. Afterwards, the electrodes were prepared, cured, and polished in the same way.

The formation of the nickel hydroxide sensor with GO was carried out in a similar way to that previously reported [30]. First, a 1 mg/mL GO solution was prepared by dilution within a 0.067 M phosphate buffer solution and submitted to exhaustive magnetic stirring. Subsequently, the electrodeposition and reduction of GO was undertaken via cyclic voltammetry, involving 10 successive scans over a potential range from −1.5 V to 0.5 V, employing a scan rate of 10 mV/s. The comparison of GEC with and without electroreduced graphene oxide (ERGO) is presented in the supplementary information in Figure S2. Next, after the deposition of the ERGO, the deposition of $Ni(OH)_2$ was conducted through cyclic voltammetry, involving a series of 15 scans in a potential range from −0.2 V to 1.0 V, using a scan rate of 100 mV/s. The electrolytic solution for this process consisted of 0.5 M KCl, 0.1 M HCl, 0.5 mM $K_3Fe(CN)_6$, and 1 mM $Ni(NO_3)_2$.

Finally, prior to their utilization, all electrodes were subjected to a stabilization step via cyclic voltammetry, consisting of carrying out several scans in a 0.1 M NaOH solution in the potential range from −1.0 V to 1.0 V at a scan rate of 100 mV/s.

2.4. Characterization by Scanning Electron Microscopy

GECs modified with metal NPs were imaged using a MERLIN field emission scanning electron microscope (FE-SEM) from Zeiss. To complement the morphological information, an energy dispersive X-ray spectroscopy (EDX) module, model Oxford Instruments X-MAX (20 mm^2), was used to obtain the comprehensive elemental analysis. Subsequently, for the determination of particle dimensions, IMAGEJ software (v. 1.53. t) was employed [31].

2.5. Samples Preparation

All measurements of alcohol standard solutions were carried in 0.1 M NaOH, necessary to observe electrocatalyis; consequently, all stock solutions were prepared in the same media.

On the one side, solutions of increasing concentration of each alcohol were prepared from the stock solutions in NaOH and measured under the above conditions to build the corresponding calibration curves for each compound. From those, their analytical response was further characterized in terms of linearity, sensitivity, LOD, reproducibility, etc.

On the other side, to assess the ET potential in achieving the simultaneous quantification of glycerol, ethanol, and methanol, a set of samples consisting of mixtures of the three compounds under scrutiny were prepared. Concretely, 48 samples encompassing a concentration spectrum ranging from 0 to 4 mM for glycerol and from 0 to 40 mM for ethanol and methanol were prepared. The set of samples was partitioned into two distinct subsets of data: a training subset, formed by 27 samples (constituting 56% of the total), which were allocated according to a 3^3 factorial design, and a testing subset, formed by 21 extra samples (44% of the total dataset), which were randomly distributed across the experimental domain. The samples corresponding to the training subset were used for the construction of the ANN response model, while those of the testing subset samples served as a robust means to assess and validate the predictive capabilities of the model.

2.6. Data Processing

The chemometric analysis was performed in MATLAB 7.1 (MathWorks, Natick, MA, USA) by specific routines developed by the authors, using the Statistics and Neural networks toolboxes. PCA was used for preliminary assessment of the potential of the proposed ET to discriminate between the different compounds under scrutiny, while ANNs were used for the quantitative modelling of the data. However, given the large dimensionality of the voltammetric data, GAs were used as the feature selection tool to reduce the number of inputs to be fed to the ANN model [32,33].

3. Results and Discussion

3.1. Characterization of GEC/Metal NPs-Modified Electrodes

The surface morphology of the built electrodes was first characterized using SEM imaging, as detailed in Section 2.4. The main goal was to confirm the presence of the different synthetized nanomaterials, viz. ERGO and the metallic NPs.

Figure 1a shows the SEM image of the CuHCF-modified GEC, from which clear clusters of NPs can be observed in certain areas of the electrode surface. Statistical analysis with ImageJ of those NPs revealed that these clusters exhibit a homogeneous distribution of NPs (although some have protrusions), with an average size of 47 $\pm$ 17 nm (Figure 1b). Further confirmation of the presence of CuHCF NPs was achieved from the EDX spectrum (Figure 1c), which revealed that the surface is composed of Cu, Fe, K, and C, all the elements that could be expected from the chemical formula of copper hexacyanoferrate plus the graphite coming from the electrode.

Similarly, Figure 1d shows the SEM image corresponding to the $Ni(OH)_2$-modified GEC electrode, from which it is evident that the NPs exhibit a uniform distribution on the electrode surface. In this case, the $Ni(OH)_2$ NPs have an average size of 61 $\pm$ 16 nm (Figure 1e), with a more spherical and homogenous shape if compared to the previous one. As before, the EDX spectrum indicates the presence of Ni, O, and C (Figure 1f), therefore confirming the successful electro-synthesis of nickel hydroxide from nickel hexacyanoferrate (NiHCF), with no presence of Fe and K elements in the spectrum.

Lastly, images corresponding to the bare GEC electrodes were also taken to confirm the lack of any metallic NPs, both from the image itself as well as from the EDX analysis (Figure 2), confirming once more the successful synthesis due to the clear differences observed between the different electrodes.

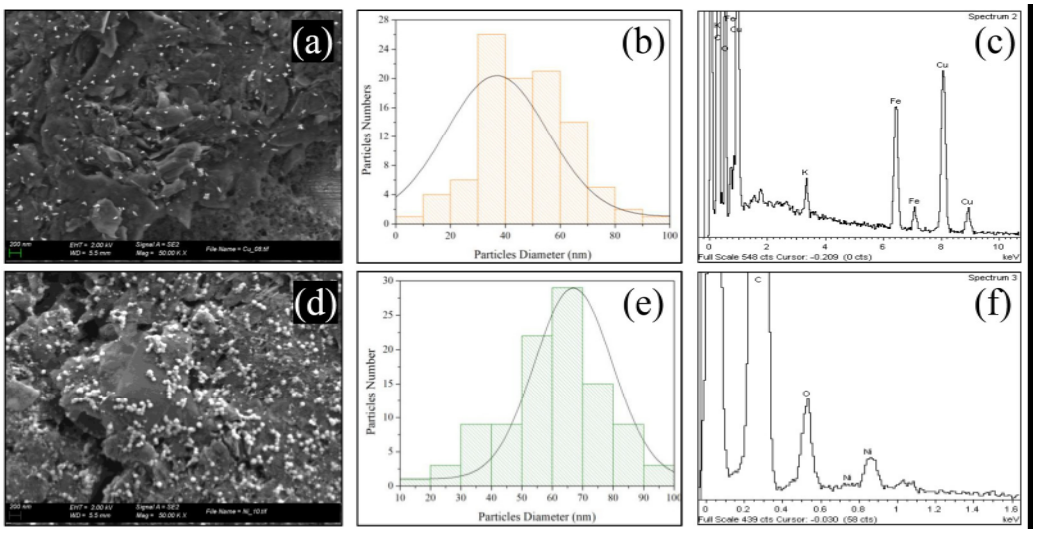

Figure 1. Characterization of the modified electrodes with (**a**–**c**) CuHCF and (**d**–**f**) $Ni(OH)_2$ NPs. (**a**,**d**) SEM image, (**b**,**e**) histograms of the size distribution of the NPs, and (**c**,**f**) EDX analysis.

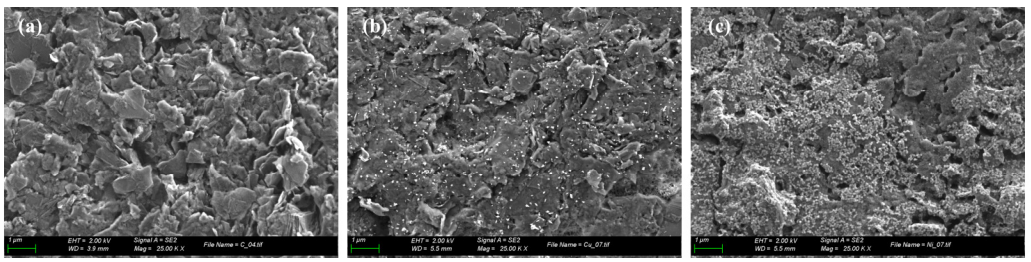

Figure 2. SEM images of (**a**) bare GEC electrode, in comparison to the same electrode modified with (**b**) CuHCF and (**c**) $Ni(OH)_2$ NPs.

3.2. Voltammetric Responses of the Electrodes

Prepared bare GEC electrodes were first tested in a 5 mM $[Fe(CN)_6]^{3/4-}$ solution containing 1 M KCl to assess their electrochemical performance, showing good reproducibility between them (Figure 3). Next, two distinct electrodes were modified, each featuring the incorporation of specific NPs: copper hexacyanoferrate and nickel hydroxide.

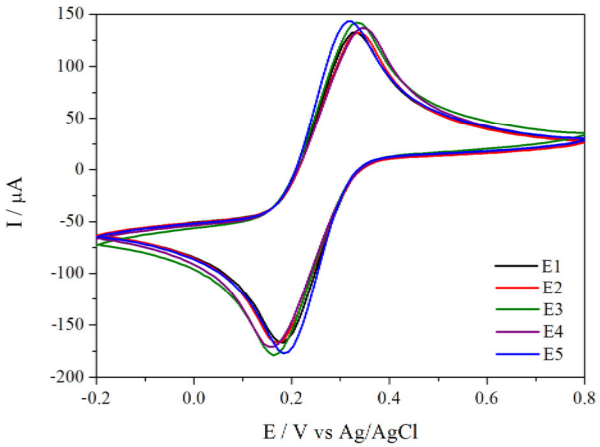

Figure 3. Cyclic voltammograms of five different GEC electrodes in a 5 mM solution of $[Fe(CN)_6]^{3/4-}$ in 1 M of KCl.

The next step was to examine the voltammetric response of each of the electrodes towards the individual compounds under study. This was conducted to ensure that a voltammetric response was obtained for each of the compounds, but, more importantly when developing an ET, that sufficiently distinct signals are obtained between the different electrodes, thereby ensuring that valuable data are generated for the construction of the multivariate calibration model. In this direction, individual standard solutions of glycerol, ethanol, and methanol were analyzed as described in Section 2.2, and the resulting voltammograms are shown in Figure 4.

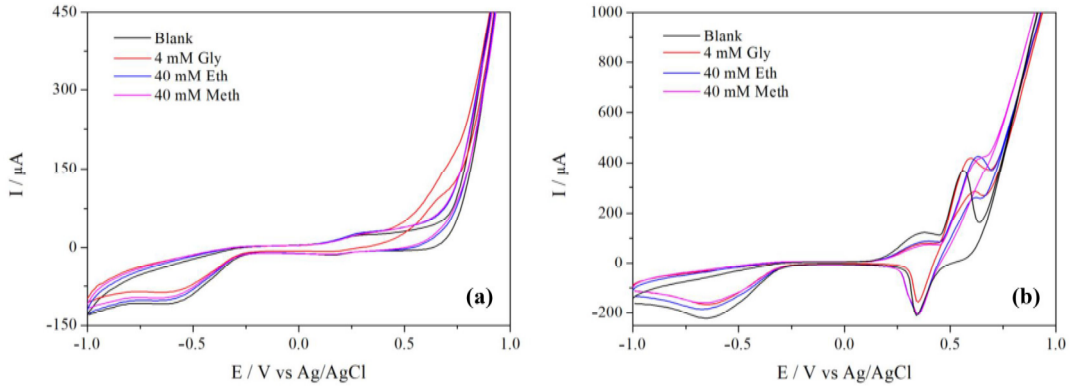

Figure 4. Example of the different voltammograms obtained with GEC sensors modified with (**a**) CuHCF and (**b**) ERGO/$Ni(OH)_2$. All solutions were prepared in 0.1 M NaOH, and the concentrations for the different alcohols were as follows: 4 mM of glycerol (Gly), 40 mM of ethanol (Eth), and 40 mM of methanol (Meth).

Figure 4a illustrates the voltammograms of the CuHCF-modified electrode. Notably, the voltammogram recorded in a solution containing 4 mM of glycerol exhibited a marked alteration at a potential *ca.* 0.65 V (vs. Ag/AgCl), accompanied by the emergence of an anodic shoulder, while for ethanol and methanol, a minimal increase in current was observed. Despite the NPs being composed of CuHCF, as confirmed by SEM-EDX analysis, the sensor's behavior resembles that of copper oxide. This convergence is attributed to the fact that, in alkaline solutions such as sodium hydroxide, CuHCF undergoes a redox process, resulting in the formation of CuO and CuOOH. During the anodic process, Cu NPs can be oxidized into CuO or CuOOH, and based on previous reports, it is plausible that the Cu^{III}/Cu^{II} redox couple plays a pivotal role in the oxidation of alcohols [34–36].

Likewise, Figure 4b shows the response of the electrode modified with ERGO/$Ni(OH)_2$ towards the three alcohols, exhibiting an increase in current for all alcohols at a potential *ca.* 0.65 V (vs. Ag/AgCl). Curiously, these changes in the anodic peak currents are concomitant with a simultaneous change in the cathodic current. These findings strongly indicate that the Ni^{III}/Ni^{II} redox couple, in the form of $Ni(OH)_2$ and NiOOH, can catalyze the electrooxidation of alcohols [37,38]. The potential electrode mechanisms taking place in these reactions have been detailed in Table S1 (supplementary information).

To better assess the cross-response of the different electrodes against the different compounds, previously shown voltammograms were submitted to PCA. The resulting score plot is presented in Figure 5. As can be seen, the accumulated explained variance reaches a value of *ca.* 89.7%; a value close to 100% indicates that most of the original data variance is now represented with only these two principal components (PCs). Furthermore, it can be noted how each of the compounds is grouped on clear clusters, easily distinguishable one from the other. Accordingly, based on the voltammetric profiles and the PCA score plot, it is safe to say that the initial selection of sensors holds the potential to tackle the simultaneous determination of the three alcohols.

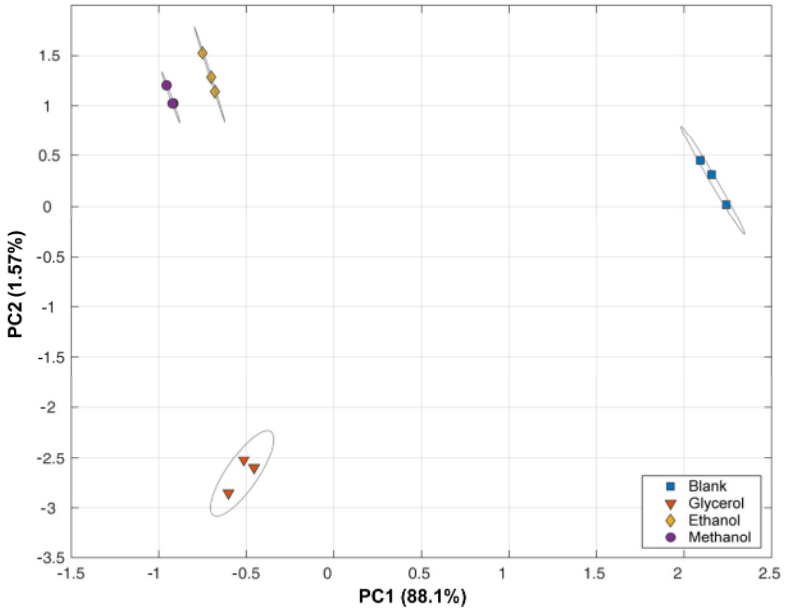

Figure 5. Scores plot of the first two principal components obtained from the PCA of the voltametric responses of the modified sensors towards: (■) Blank, (▼) glycerol, (●) ethanol, and (♦) methanol. Ellipses plotted correspond to 95% confidence limits for each of the clusters.

However, prior to that, the analytical characterization of sensors performance was carried out. On the one side, this is needed to assess the linear behavior (and response range) of the different sensors and also to corroborate that different sensitivities were actually shown between them, this being an important condition to assure the resolution of the considered compounds. These will, in turn, allow us to later define the experimental domain for the quantitative experiment. On the other side, the sensors' repeatability will also be assessed, a critical feature when working with ETs, as the building of the response models normally requires performing a large number of consecutive measurements.

The analytical stability of the sensors for long time application (evaluated in terms of their relative standard deviation, %RSD) was estimated using a mixed solution with 5 mM glycerol, 50 mM ethanol, and 50 mM methanol. A total of 27 measurements were conducted, yielding %RSD values of 2.70%, 5.02%, and 2.76% for CuHCF, $Ni(OH)_2$, and-GEC electrodes, respectively. The %RSD for the modified electrodes (CVs are shown in supplementary information, Figure S3) was measured, resulting in 4.18% and 5.51% for the CuHCF- and $Ni(OH)_2$-modified electrodes, respectively. With regard the third electrode used, the reproducibility of construction can be derived from the superimposed voltammograms in Figure 3, whereas the variability of the maximum oxidation currents was 3.85%. In addition to this, the %RSD for three sequential measurements with different alcohols was determined. For glycerol at a concentration of 4 mM, the %RSD for the CuHCF- and $Ni(OH)_2$-modified electrodes was 3.96% and 6.70%, respectively. For the $Ni(OH)_2$-modified electrode in the presence of 40 mM ethanol and methanol, the RSD was 3.10% and 2.13%, respectively.

Next, once their stability was confirmed, calibrations curves for the different alcohols in 0.1 M NaOH solution were built to fully characterize the sensors.

In all cases, there was a linear increase in the anodic current with increasing glycerol concentration, with all sensors responding accurately and linearly (Table 1). However, for ethanol and methanol, the CuHCF-modified sensor faced challenges in achieving good linear responses at low concentrations. for the $Ni(OH)_2$-modified sensor, the similarity between ethanol and methanol molecular structures, with ethanol succeeding methanol in the molecular chain, can be considered as the reason for the considerable similarity in the responses, as shown in Table 1. Though this might not be an ideal situation, the use of ANNs, combining both linear and non-linear functions, can assist in the successful mod-

elling of the observed non-linear behavior, allowing us to achieve the correct quantification of the different compounds.

Table 1. Calibration data for the individual calibrations of glycerol, ethanol, and methanol employing the different NPs-modified sensors.

Sensor	Compound	LOD (mM)	Sensitivity (μM/mM)	Concentration Range (mM)
CuHCF	Glycerol	0.28	6.6 ± 0.6	1.0–4.0
	Ethanol	n.d. [1]	n.d. [1]	10–40
	Methanol	n.d. [1]	n.d. [1]	10–40
$Ni(OH)_2$	Glycerol	0.09	0.31 ± 0.07	1.0–4.0
	Ethanol	2.73	9.1± 1.6	10–40
	Methanol	2.16	7.2 ± 0.9	10–40

[1] n.d.: not determined. Uncertainties corresponding to different days (n = 4).

3.3. ANN Model

The last step of this study involved building the ANN model to achieve the simultaneous quantitative determination of glycerol, ethanol, and methanol in biodiesel. To this end, the set of samples described in Section 2.5 were measured under the same conditions as in previous experiments, recording a complete cyclic voltammogram for each of the electrodes.

However, before constructing the quantification model, it is essential to perform a preprocessing step to reduce the high dimensionality of the data, especially when using ANNs. This step is crucial for preventing the under-determination issue that can occur with large, overly complex ANNs, while at the same time, it significantly decreases the time and memory required for the modeling process [39]. Additionally, this step generally enhances the model performance and generalization ability thanks to the removal of redundant input data and the reduction of the model's complexity, thereby mitigating the risk of overfitting [32,39].

In our case, this was achieved by means of GAs, which were used as an iterative feature selection tool. In this manner, from the original data, only sixty-two final current values from the three sensors were selected and fed to the ANN model. In addition, the ANN topology was optimized to find the best configuration that optimizes its performance, which in our case had 62 neurons (corresponding to the selected currents with GAs) in the input layer, 4 neurons and a *tansig* transfer function in the hidden layer, and three neurons and a *satlins* transfer function in the output layer.

Subsequently, the performance of the developed model was assessed by building comparison graphs of predicted vs. expected concentration values for both subsets (training and testing, Figure 6), showing a satisfactory trend close to the ideal one, especially in the case of glycerol. To numerically assess the performance of the ANN model, the linear regression parameters of the comparison lines were assessed. As could be deduced from the plot, the general trend in all cases was satisfactory, as the intercept and slope values were close to the ideal values (viz., 0 and 1, respectively). In the case of ethanol and methanol, although the performance was not as good as for glycerol, with an observed dispersion larger than desirable for a quantitative application, correlations were still significant, and still good enough for a semi-quantitative approach. In this respect, it should be considered that the challenging situation is the quantification of methanol and ethanol separately with just a simple electrochemical measurement, given their similarity; this scenario highlights the significant improvement attained thanks to the use of the advanced data treatment proposed model.

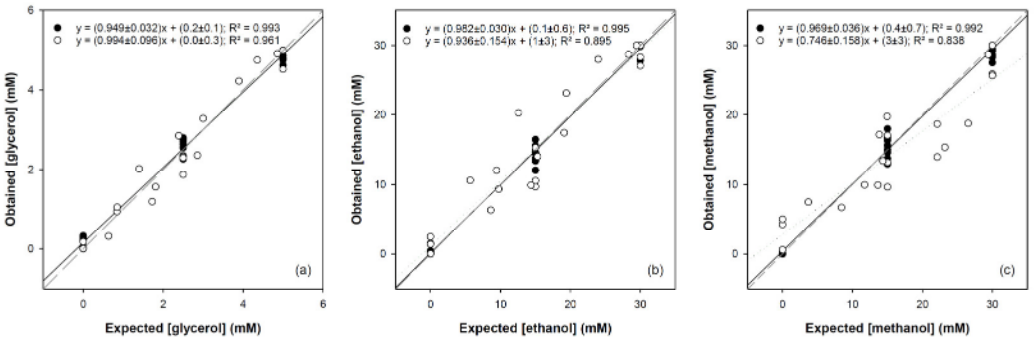

Figure 6. Modeling ability of the optimized GA-ANNs. Comparison graphs of obtained vs. expected concentrations for (**a**) glycerol, (**b**) ethanol, and (**c**) methanol, for both the training (●, solid line) and testing subsets (○, dotted line). Dashed line corresponds to the ideal comparison line (y = x).

4. Conclusions

The application of an ET formed by GECs modified with different metal NPs is described for the detection and quantification of glycerol in the presence of ethanol and methanol; a scenario very relevant during the production of biodiesel. Glycerol, ethanol, and methanol are typical substances representative of residual contaminants in the biodiesel transesterification process.

First, the successful synthesis of Cu and Ni NPs from simple and straightforward procedures should be highlighted, synthesis that was confirmed through SEM imaging. Second, the synthetized NPs were utilized as electrocatalysts for the modification of voltammetric electrodes, showing significant catalytic properties and allowing us to obtain individual calibration curves based on the peak height of the voltammetric responses for glycerol, ethanol, and methanol. These calibration curves exhibited notable correlations within the linear range of each respective individual analyte system. Nonetheless, practical implementation in biodiesel analysis was found to be constrained due to proximity of the peak potentials in samples containing multiple analytes. Hence, the integration of an ANN response model offers an improved estimation strategy, as it combines responses from various sensors and effectively compensates for disparities in the voltammetric responses to distinct compounds. In this regard, further efforts will be directed in improving the voltammetric discrimination of methanol and ethanol.

Overall, the proposed approach herein holds huge potential for the determination of glycerol and other alcohols in biodiesel samples, showing some significant advantages over other approaches, such as its low-cost, short analysis time, and portability. Most significantly, this method provides the possibility of resolving these highly related three substances without the need to use enzymes and their specificity.

Supplementary Materials: The following supporting information can be downloaded at: https://www.mdpi.com/article/10.3390/chemosensors12090173/s1, Figure S1. SEM images of synthetized graphene oxide (GO) in different magnitudes (a) 50x and (b) 6000x. (c) Raman spectrum of GO showing D, G, 2D and D+D′ bands. (d) FT-IR spectrum of GO showing several informative IR band positions; Figure S2. Cyclic voltammograms of GEC electrodes with and without GO in a 5 mM solution of [Fe(CN)6]3/4- in 1 M KCl background media; Figure S3. Cyclic voltammograms obtained with three different GEC sensors modified with (a) CuHCF and (b) ERGO/Ni(OH)2 in solution of 0.1 M NaOH; Table S1. Table summarizing the catalytic mechanisms of oxidations of glycerol, methanol and ethanol with the modified electrodes used in the study.

Author Contributions: Conceptualization, A.C.d.S., L.L.P. and M.d.V.; Funding acquisition, M.d.V.; Investigation, J.P.J.d.O. and M.B.-S.-E.; Methodology, M.B.-S.-E. and M.d.V.; Resources, M.B.-S.-E. and M.d.V.; Software, X.C.; Supervision, A.C.d.S. and L.L.P.; Writing—original draft, J.P.J.d.O.; Writing—review and editing, X.C. and M.d.V. All authors have read and agreed to the published version of the manuscript.

Funding: This research was funded by the Spanish Ministry of Science and Innovation, MCIN/AEI/10.1303/501100011033, through the project PID2022-136709OB-C21, the Fundação de Amparo à Pesquisa do Estado de São Paulo (FAPESP) (Proc. 2017/17559-1, Proc. 2019/02343-9 and Proc. 2017/09123-9) and the Generalitat of Catalunya (Project 2021 SGR 00124).

Institutional Review Board Statement: Not applicable.

Informed Consent Statement: Not applicable.

Data Availability Statement: Data will be made available upon specific request to authors.

Conflicts of Interest: The authors declare no conflicts of interest.

References

1. Mumtaz, M.W.; Adnan, A.; Mukhtar, H.; Rashid, U.; Danish, M. Biodiesel production through chemical and biochemical transesterification: Trends, technicalities, and future perspectives. In *Clean Energy for Sustainable Development*; Rasul, M.G., Azad, A.K., Sharma, S.C., Eds.; Academic Press: London, UK, 2017; pp. 465–485.
2. Babadi, A.A.; Rahmati, S.; Fakhlaei, R.; Barati, B.; Wang, S.; Doherty, W.; Ostrikov, K. Emerging technologies for biodiesel production: Processes, challenges, and opportunities. *Biomass Bioenerg.* **2022**, *163*, 106521. [CrossRef]
3. Ruschel, C.F.C.; Ferrão, M.F.; Santos, F.P.D.; Samios, D. Otimização do processo de transesterificação em duas etapas para produção de biodiesel através do planejamento experimental Doehlert. *Quim. Nova* **2016**, *39*, 267–272.
4. Veljković, V.B.; Banković-Ilić, I.B.; Stamenković, O.S. Purification of crude biodiesel obtained by heterogeneously-catalyzed transesterification. *Renew. Sustain. Energ. Rev.* **2015**, *49*, 500–516. [CrossRef]
5. Sheldon, R.A. Green and sustainable manufacture of chemicals from biomass: State of the art. *Green Chem.* **2014**, *16*, 950–963. [CrossRef]
6. Stojković, I.J.; Stamenković, O.S.; Povrenović, D.S.; Veljković, V.B. Purification technologies for crude biodiesel obtained by alkali-catalyzed transesterification. *Renew. Sustain. Energ. Rev.* **2014**, *32*, 1–15. [CrossRef]
7. Jaganjac, M.; Prah, I.O.; Cipak, A.; Cindric, M.; Mrakovcic, L.; Tatzber, F.; Ilincic, P.; Rukavina, V.; Spehar, B.; Vukovic, J.P.; et al. Effects of bioreactive acrolein from automotive exhaust gases on human cells in vitro. *Environ. Toxicol.* **2012**, *27*, 644–652. [CrossRef]
8. Heiden, R.W.; Schober, S.; Mittelbach, M. Solubility limitations of residual steryl glucosides, saturated monoglycerides and glycerol in commercial biodiesel fuels as determinants of filter blockages. *J. Am. Oil Chem.* **2021**, *98*, 1143–1165. [CrossRef]
9. Maduraiveeran, G.; Sasidharan, M.; Ganesan, V. Electrochemical sensor and biosensor platforms based on advanced nanomaterials for biological and biomedical applications. *Biosens. Bioelec.* **2018**, *103*, 113–129. [CrossRef] [PubMed]
10. Brainina, K.; Stozhko, N.; Bukharinova, M.; Vikulova, E. Nanomaterials: Electrochemical properties and application in sensors. *Phys. Sci. Rev.* **2018**, *3*, 20188050.
11. Baranwal, J.; Barse, B.; Gatto, G.; Broncova, G.; Kumar, A. Electrochemical sensors and their applications: A review. *Chemosensors* **2022**, *10*, 363. [CrossRef]
12. Ferrag, C.; Kerman, K. Grand challenges in nanomaterial-based electrochemical sensors. *Front. Sens.* **2020**, *1*, 583822. [CrossRef]
13. Squissato, A.L.; Almeida, E.S.; Silva, S.G.; Richter, E.M.; Batista, A.D.; Munoz, R.A.A. Screen-printed electrodes for quality control of liquid (bio)fuels. *TrAC-Trend. Anal. Chem.* **2018**, *108*, 210–220. [CrossRef]
14. Arévalo, F.J.; Osuna-Sánchez, Y.; Sandoval-Cortés, J.; Di Tocco, A.; Granero, A.M.; Robledo, S.N.; Zon, M.A.; Vettorazzi, N.R.; Martínez, J.L.; Segura, E.P.; et al. Development of an electrochemical sensor for the determination of glycerol based on glassy carbon electrodes modified with a copper oxide nanoparticles/multiwalled carbon nanotubes/pectin composite. *Sensor Actuat. B-Chem.* **2017**, *244*, 949–957. [CrossRef]
15. Honório, G.G.; da Cunha, J.N.; dos Santos Castro Assis, K.L.; de Aguiar, P.F.; de Andrade, D.F.; de Souza, C.G.; d'Avila, L.A.; Archanjo, B.S.; Achete, C.A.; Pradelle, R.N.C.; et al. Free glycerol determination in biodiesel samples using palladium nanoparticles modified glassy carbon electrode associated with solid phase extraction. *J. Solid State Electr.* **2019**, *23*, 3057–3066. [CrossRef]
16. Paiva, V.M.; Assis, K.L.d.S.C.; Archanjo, B.S.; Ferreira, D.R.; Senna, C.A.; Ribeiro, E.S.; Achete, C.A.; D'Elia, E. Electrochemical analysis of free glycerol in biodiesel using reduced graphene oxide and gold/palladium core-shell nanoparticles modified glassy carbon electrode. *Processes* **2021**, *9*, 1389. [CrossRef]
17. Assis, K.L.d.S.C.; Archanjo, B.S.; Achete, C.A.; D'Elia, E. A new sensor based on reduced graphene oxide/Au nanoparticles for glycerol detection. *Mater. Res.* **2020**, *23*, e20190513. [CrossRef]
18. Ravipati, M.; Badhulika, S. Nanoporous copper–metal organic framework microneedles on nickel foam as a bifunctional electrocatalyst for glycerol fuel cell and electrochemical glycerol detection in biodiesel. *ACS Appl. Nano Mater.* **2024**, *7*, 7277–7288. [CrossRef]
19. Cetó, X.; Voelcker, N.H.; Prieto-Simón, B. Bioelectronic tongues: New trends and applications in water and food analysis. *Biosens. Bioelec.* **2016**, *79*, 608–626. [CrossRef]
20. Ciosek, P.; Wroblewski, W. Sensor arrays for liquid sensing-electronic tongue systems. *Analyst* **2007**, *132*, 963–978. [CrossRef]
21. Cetó, X.; del Valle, M. Electronic tongue applications for wastewater and soil analysis. *iScience* **2022**, *25*, 104304. [CrossRef]

22. Vijayan, A.; Prakash, J. Emerging analytical methods for quantitative determination of biofuel-petroleum blend composition. *Anal. Lett.* **2024**, 1–18. [CrossRef]
23. Mazivila, S.J. Trends of non-destructive analytical methods for identification of biodiesel feedstock in diesel-biodiesel blend according to european commission directive 2012/0288/EC and detecting diesel-biodiesel blend adulteration: A brief review. *Talanta* **2018**, *180*, 239–247. [CrossRef] [PubMed]
24. Moro, M.K.; dos Santos, F.D.; Folli, G.S.; Romão, W.; Filgueiras, P.R. A review of chemometrics models to predict crude oil properties from nuclear magnetic resonance and infrared spectroscopy. *Fuel* **2021**, *303*, 121283. [CrossRef]
25. de Sá, A.C.; Cipri, A.; González-Calabuig, A.; Stradiotto, N.R.; del Valle, M. Resolution of galactose, glucose, xylose and mannose in sugarcane bagasse employing a voltammetric electronic tongue formed by metals oxy-hydroxide/MWCNT modified electrodes. *Sensor Actuat. B-Chem.* **2016**, *222*, 645–653. [CrossRef]
26. Hummers, W.S., Jr.; Offeman, R.E. Preparation of graphitic oxide. *J. Am. Chem. Soc.* **1958**, *80*, 1339. [CrossRef]
27. Aceta, Y.; del Valle, M. Graphene electrode platform for impedimetric aptasensing. *Electrochim. Acta* **2017**, *229*, 458–466. [CrossRef]
28. Ma, X.-H.; Jia, W.; Wang, J.; Zhou, J.-H.; Wu, Y.-D.; Wei, Y.-Y.; Zi, Z.-F.; Dai, J.-M. Synthesis of copper hexacyanoferrate nanoflake as a cathode for sodium-ion batteries. *Ceram. Int.* **2019**, *45*, 740–746. [CrossRef]
29. Olivé-Monllau, R.; Baeza, M.; Bartrolí, J.; Céspedes, F. Novel amperometric sensor based on rigid near-percolation composite. *Electroanalysis* **2009**, *21*, 931–938. [CrossRef]
30. de Oliveira, J.P.J.; de Sá, A.C.; Sousa, M.S.P.; Hiranobe, C.T.; Paim, L.L. A facile controlled-synthesis method of nanoparticles of nickel oxide/hydroxide anchored in graphite/rgo for alcohol oxidation. *ECS J. Solid State Sci. Technol.* **2021**, *10*, 011001. [CrossRef]
31. Schneider, C.A.; Rasband, W.S.; Eliceiri, K.W. NihIMAGE to IMAGEJ: 25 years of image analysis. *Nat. Methods* **2012**, *9*, 671–675. [CrossRef]
32. Cetó, X.; Céspedes, F.; del Valle, M. Comparison of methods for the processing of voltammetric electronic tongues data. *Microchim. Acta* **2013**, *180*, 319–330. [CrossRef]
33. Richards, E.; Bessant, C.; Saini, S. Optimisation of a neural network model for calibration of voltammetric data. *Chemometr. Intell. Lab.* **2002**, *61*, 35–49. [CrossRef]
34. Dantas, L.M.F.; De Souza, A.P.R.; Castro, P.S.; Paixão, T.R.L.C.; Bertotti, M. SECM studies on the electrocatalytic oxidation of glycerol at copper electrodes in alkaline medium. *Electroanalysis* **2012**, *24*, 1778–1782. [CrossRef]
35. Ganesh, V.; Latha Maheswari, D.; Berchmans, S. Electrochemical behaviour of metal hexacyanoferrate converted to metal hydroxide films immobilized on indium tin oxide electrodes—Catalytic ability towards alcohol oxidation in alkaline medium. *Electrochim. Acta* **2011**, *56*, 1197–1207. [CrossRef]
36. Heli, H.; Jafarian, M.; Mahjani, M.G.; Gobal, F. Electro-oxidation of methanol on copper in alkaline solution. *Electrochim. Acta* **2004**, *49*, 4999–5006. [CrossRef]
37. Shabnam, L.; Faisal, S.N.; Roy, A.K.; Gomes, V.G. Nickel-nanoparticles on doped graphene: A highly active electrocatalyst for alcohol and carbohydrate electrooxidation for energy production. *ChemElectroChem* **2018**, *5*, 3799–3808. [CrossRef]
38. Berchmans, S.; Gomathi, H.; Rao, G.P. Electrooxidation of alcohols and sugars catalysed on a nickel oxide modified glassy carbon electrode. *J. Electroanal. Chem.* **1995**, *394*, 267–270. [CrossRef]
39. Despagne, F.; Massart, D.L. Neural networks in multivariate calibration. *Analyst* **1998**, *123*, 157R–178R. [CrossRef]